NACA TN 4093
10427

TECH LIBRARY KAFB, NM
0066964

NATIONAL ADVISORY COMMITTEE FOR AERONAUTICS

TECHNICAL NOTE 4093

INVESTIGATION OF HEAT TRANSFER FROM A STATIONARY AND ROTATING CONICAL FOREBODY

By Robert S. Ruggeri and James P. Lewis

Lewis Flight Propulsion Laboratory
Cleveland, Ohio

Washington
October 1957

AFMDC
TECHNICAL LIBRARY
AFL 2811

TECH LIBRARY KAFB, NM

0066964

NATIONAL ADVISORY COMMITTEE FOR AERONAUTICS

TECHNICAL NOTE 4093

INVESTIGATION OF HEAT TRANSFER FROM A STATIONARY AND ROTATING CONICAL FOREBODY

By Robert S. Ruggeri and James P. Lewis

4214

CR-1

SUMMARY

The convective heat transfer from the surface of a conical forebody having a hemispherical nose, an included angle of approximately 30°, and a maximum diameter of 18.9 inches was investigated in a wind tunnel for both stationary and rotating operation. The range of test conditions included free-stream velocities up to 400 feet per second, rotational speeds up to 1200 rpm, and angles of attack of 0° and 6°. Both a uniform surface temperature and a uniform heater input power density were used.

The Nusselt-Reynolds number relations provided good correlation of the heat-transfer data for the complete operating range at 0° angle of attack with and without spinner rotation, and for 6° angle of attack with rotation. Rotational speeds up to 1200 rpm had no apparent effect on the heat-transfer characteristics of the spinner. The results obtained at 6° angle of attack with rotation were essentially the same as those obtained at 0° angle of attack without rotation. The experimental heat-transfer characteristics in the turbulent flow region were consistently in closer agreement with the results predicted for a two-dimensional body than with those predicted for a cone. For stationary operation at 6° angle of attack, the measured heat-transfer coefficients in the turbulent flow region were from 6 to 13 percent greater on the lower surface (windward side) than on the upper surface (sheltered side) for corresponding surface locations. The spinner-nose geometry appeared to cause early boundary-layer transition. Transition was inititated at a fairly constant Reynolds number (based on surface distance from nose) of 8.0×10^4. Transition was completed at Reynolds numbers less than 5.0×10^5 for all conditions investigated.

INTRODUCTION

Fundamental information on the heat-transfer and boundary-layer characteristics of stationary and rotating simple bodies of revolution is needed to design icing protection systems for all-weather aircraft.

Examples of simple three-dimensional bodies used as aircraft components are radomes, forward sections of external stores, propeller spinners for turboprop engines, and jet-engine accessory housings. Several theoretical and experimental heat-transfer studies have been made for such bodies, but the data are generally limited to specific problems, such as supersonic flight, small or zero angles of attack, or zero rotational speeds.

As part of a general experimental program conducted at the NACA Lewis laboratory on icing protection for bodies of revolution, the present investigation is a study of the heat transfer from the surface of a conical forebody in clear air for low subsonic flight speeds, with and without rotation, and for angle-of-attack operation. This work is an extension of heat-transfer studies reported in references 1 and 2 for two ellipsoidal bodies of revolution having fineness ratios of 3.0 and 2.5.

SYMBOLS

A,B,C,D, E,F,G,H	heater elements (fig. 2)
d	model nosecap diameter, ft
c_p	specific heat at constant pressure, Btu/(lb)(°F)
g	gravitational constant, 32.2 ft/sec^2
h	convective heat-transfer coefficient, Btu/(hr)(sq ft)(°F)
k	thermal conductivity, Btu/(hr)(sq ft)(°F/ft)
Nu_d	Nusselt number at stagnation point, hd/k_a, dimensionless
Nu_s	local Nusselt number, hs/k_a, dimensionless
Pr	Prandtl number based on free-stream stagnation air temperature properties, $3600g\mu c_p/k_a$, dimensionless
Q	rate of heat input per unit area, Btu/(hr)(sq ft)
Q_{Al}	rate of heat conduction between heater elements through aluminum skin, Btu/(hr)(sq ft)
Q_i	rate of heat flow to body interior, Btu/(hr)(sq ft)
Q_s	rate of heat transfer from external surface, Btu/(hr)(sq ft)
Re_d	Reynolds number based on nosecap diameter, $U_0\rho d/\mu$, dimensionless

Re_s local surface Reynolds number, $U_s \rho s/\mu$, dimensionless

s surface distance from nose, ft (except as noted)

t_d datum or unheated surface temperature, °F

t_h heater interior temperature as measured by thermocouple h (fig. 2), °F

t_i temperature of heater insulation on interior side as measured by thermocouple i (fig. 2), °F

t_s spinner surface temperature as measured by thermocouple s (fig. 2), °F

U_s local velocity on spinner surface, ft/sec

U_0 free-stream air velocity, ft/sec or knots (as noted)

α angle of attack, deg

μ absolute viscosity of air, lb-sec/sq ft

ρ density of air, (lb)(sec^2)/ft^4

τ conical shell thickness, ft

Subscripts:

a air

Al aluminum skin

av value averaged over area of heater element

s surface condition

APPARATUS AND PROCEDURE

The study of heat transfer from the surface of a conical forebody was conducted in the 6- by 9-foot test section of the Lewis icing research tunnel. Figure 1 is a photograph of the model installed in the tunnel. The faired afterbody and its related equipment for obtaining temperature and pressure measurements with rotation is the same as that used in previous heat-transfer studies of ellipsoids (refs. 1 and 2). The 18.9-inch maximum diameter of the conical model was faired to the 20-inch minimum diameter of the afterbody by a transition piece that rotated with the model.

4274

CR-1 back

The conical model proper, hereinafter referred to as a "cone" or "spinner", had an axial length of 35 inches and was constructed of 0.061-inch aluminum spun to the desired shape. The nose, or apex, of the cone was rounded to a 1/2-inch radius and the spinner surface was slightly convex (bulged), deviating from a true conical surface by approximately 0.6 inch at the midpoint. Approximately 1000 square inches of heated surface area were provided by means of internal electric heaters of the blanket type. Although the spinner model was not a true cone, it was considered adequately representative, especially for a practical installation employing blanket-type heaters. It should be stated that the model, supplied by the U. S. Air Force, was not designed and built for the specific purpose of obtaining detailed basic heat-transfer information, but rather was a production article in many respects.

A schematic drawing of the spinner model, heater layout, details of heater construction, and thermocouple cross-sectional locations are shown in figure 2. The thermocouples located within the heater proper were used to determine heat losses to the cone interior. The area and surface length of each of the eight heater segments are presented in table I. Each heater operated on a single electrical circuit to permit selective control of power density and axial surface temperature distribution. The longitudinal heaters G and H constitute one of a pair of parting strips (diametrically opposite each other) which were incorporated into the design for use in subsequent icing studies. Heater segment F contained limited instrumentation and, for the present investigation, was considered a guard heater only. The heater materials and methods of construction were identical to those reported in reference 1. Input power to each heater segment was measured by means of a voltmeter and ammeter and checked by a recording wattmeter. All thermocouples (copper-constantan) were located in a meridional plane midway between the parting strips.

Surface-pressure-distribution measurements were obtained at nominal free-stream velocities of 250 and 375 feet per second (148 and 222 knots, respectively); rotational speeds of 0, 600, and 1200 rpm; and angles of attack of 0°, 3°, and 6°. The measurements were made on a spare spinner shell identical to, insofar as practicable, the actual heated model. Rotation was in a clockwise direction looking upstream, and changes in angle of attack occurred in the horizontal plane.

All heat-transfer data were obtained for steady-state conditions. Because heat transfer is affected by distributions in surface temperature, data were obtained for two heating conditions: uniform surface temperature distribution and uniform input power density to all heater segments. The temperature distributions yielded by these two heating conditions are considered to bracket those most likely to be used in practical heated-spinner applications. For the uniform surface temperature condition, a surface temperature approximately 100° F greater than the unheated equilibrium (datum) temperature was employed wherever possible. For this case

the input powers to heaters G and H were set to an approximate average of power densities supplied adjacent circumferential heaters. For uniform power distribution, nominal power densities of 9 and 10 watts per square inch were supplied to all heater segments. Heat-transfer data were taken at free-stream velocities from 275 to 400 feet per second; four spinner rotational speeds from 0 to 1200 rpm; angles of attack of 0° and 6°, and a nominal free-stream total temperature of 0° F. Unheated, or datum, temperatures were measured at the beginning of each test run or condition.

4274

METHOD OF ANALYSIS

Experimental data. - The experimental results are presented in terms of the surface temperature rise above equilibrium surface temperature $(t_s - t_d)$, the convective heat transfer coefficient h, and the Nusselt parameter Nu_s. The heat-transfer coefficient is defined as

$$h = \frac{Q_s}{t_s - t_d} \tag{1}$$

where

$$Q_s = Q - Q_i \pm Q_{Al} \tag{1a}$$

and

$$Q_{Al} = \pm k_{Al}\tau\left(\frac{\partial^2 t_s}{\partial s^2} + \frac{1}{s}\frac{\partial t_s}{\partial s}\right) \tag{1b}$$

The heat flow paths assumed for the calculations are shown in figure 3. The external convective heat-transfer coefficient h was evaluated on the basis of an effective local heat dissipation from the external surface, neglecting in most cases longitudinal and circumferential heat conduction through the model skin Q_{Al}, but in all cases accounting for heat loss to the cone interior Q_i. The heat loss to the interior of the model was determined from the relation

$$Q_i = 28.8(t_h - t_i), \text{ Btu/(hr)(sq ft)} \tag{2}$$

The effective thermal conductivity of 28.8 Btu/(hr)(sq ft)($^{\circ}$F) for the 0.062-inch-thick insulating layer of silastic and glass cloth between the inner thermocouples (h and i in fig. 2) was experimentally determined on an instrumented sample of the heater. The heat loss to the interior was subtracted from the heater-segment input heat density Q to obtain the effective outward local heat density at each surface thermocouple

location. The resulting convective heat-transfer coefficient is therefore regarded as an effective local coefficient rather than a true local coefficient since, by neglecting heat conduction in the aluminum skin, the exact local heat dissipation from the surface is not used. Although most of the data is presented in terms of this effective local heat-transfer coefficient, a limited amount of data was analyzed to include the effect of longitudinal heat conduction in the skin. The method of analysis is presented in detail in reference 1. Briefly, the method yields a single heat-transfer coefficient for each heater segment, based on an area-averaged value of surface temperature and external heat flow rate. The analysis was conducted only for the case of uniform heat input, since only for this condition are the values of temperature gradient considered valid. No effort was made to account for circumferential heat conduction or conduction within the heater proper.

In the calculation of the nondimensional parameters used to correlate the heat-transfer results (Nusselt, Reynolds, and Prandtl numbers), the air properties were evaluated at free-stream total temperature for ease in computation. For the conditions investigated, the choice of temperature at which air properties are evaluated affects the correlation only slightly. For spinner rotation, local velocities (fig. 4(b)) and surface distances based on an approximate helical path length were employed to calculate the Reynolds and Nusselt numbers.

Theoretical heat transfer. - The experimental results are compared with the values predicted from several different analyses. For the laminar boundary-layer region, the results are compared primarily with the values predicted by the method of Drake (ref. 3) for three-dimensional boundary layers. The analysis of Drake is applicable to bodies of revolution having both an arbitrary surface temperature distribution and an arbitrary velocity distribution (pressure gradient) in axisymmetric flow. Experimentally determined values of local velocity (fig. 4(a)) were used in these computations.

Predicted values of laminar heat transfer were also obtained from a simpler analysis wherein the predicted results of heat transfer for a flat plate are transformed into three-dimensional values for the cone. The equation for laminar flow over a flat plate is modified by $\sqrt{3.0}$ (ref. 4) to extend the results to the three-dimensional flow over a cone:

$$Nu_s = 0.575\ Re_s^{0.5}\ Pr^{1/3} \tag{3}$$

Equation (3) assumes zero pressure gradient and is strictly applicable only for the case of a supersonic cone with an attached shock wave. A comparison of the results obtained from reference 3 (Drake) and equation (3) does, however, indicate to what extent pressure gradient might affect heat transfer in the laminar region.

In the region of turbulent flow, the experimental results are compared with values predicted by the analyses of Van Driest for flat plates and cones (refs. 5 and 6, respectively). Reference 5 presents a method of determining heat transfer from a flat plate in compressible flow having zero pressure gradient and arbitrary values of surface- to free-stream temperature ratio. Turbulent heat transfer for the cone was determined by the method of reference 6 for transforming the local heat-transfer coefficients for flat plates to those for a cone at 0° angle of attack with zero pressure gradient. Theoretical flat-plate heat transfer (ref. 5) was determined for the following operating conditions: free-stream Mach number, 0.3; wall- to free-stream temperature ratio, 1.25; and Prandtl number, 0.72. These conditions correspond to those at which the bulk of the experimental data was obtained. The flat-plate values were then extended to the three-dimensional case for a cone by use of reference 6.

4274

Heat transfer at air stagnation was predicted from results obtained in two previous investigations - a theoretical study by Silbukin (ref. 7) and an experimental study by Xenakis, et al (ref. 8). Because the model had a hemispherical nosecap, the methods employed to predict heat transfer at stagnation pertain specifically to spheres. The study of Silbukin yields the following relation for stagnation heat transfer on a sphere

$$Nu_d = 1.32\ Re_d^{0.5}\ Pr^{0.4}$$

where Nu_d and Re_d are based on the diameter of the nosecap ($d = 0.0833$ ft).

RESULTS AND DISCUSSION

Velocity Distribution

The velocity distribution over the surface of the cone for zero rotation is presented in figure 4(a) in terms of the ratio of local to free-stream velocity U_s/U_0 for three angles of attack. For the conditions investigated, the sharp peak in velocity occurred at a constant value of 0.7 inch from the spinner nose, which corresponds to the point at which the cone body becomes tangent to the hemispherical nosecap. The shift in air stagnation point was found to be very small (less than 1/8 inch at 6°) and was neglected in computations involving local surface distance. The theoretically predicted velocity distribution (ref. 9) for a true 15° half-angle cone at 0° angle of attack is presented for comparison with experimental results. Measurements in a meridional plane midway between the upper and lower surfaces for 6° angle of attack (stationary) showed local velocities in this plane to be only 1.5 to 3.0 percent lower than those obtained for the upper, or sheltered, surface.

Velocity distributions with spinner rotation are presented in figure 4(b) for 0°, 3°, and 6° angles of attack. These curves are for the maximum rotational speed and minimum free-stream velocity investigated (1200 rpm and 255 ft/sec, respectively). The results show that, with spinner rotation, velocity distribution is rather insensitive to small changes in angle of attack. In addition, comparison of figures 4(b) and 4(a) shows that rotation at 0° angle of attack caused a maximum increase in local velocity of only about 5 percent at the rear of the spinner.

With rotation, the true local velocity with respect to the moving cone surface was not determined directly from experiment because the local total pressures were not measured. The true local surface velocities were therefore determined, in part, by computation. When the experimental values of local static pressure were corrected for centrifugal effects, the resulting pressure distribution was essentially the same as that obtained without rotation, which indicated negligible viscous effects. The experimental pressure distribution, in conjunction with free-stream total pressure, could therefore be used to determine the true longitudinal component of velocity. Since the local tangential velocities were known, it was possible to obtain true surface velocities by simple calculation of the resultant of these longitudinal and tangential components (fig. 4(b)).

Heat Transfer with Uniform Heat Input

Typical results. - Typical data obtained at 0° angle of attack with uniform heat input (nonuniform surface temperature) are presented in figure 5 in terms of the surface temperature rise $t_s - t_d$ and the convective heat-transfer coefficient h for two values of input power density. The data (from nonconsecutive runs) are for a stationary spinner and exemplify the general characteristics and repeatability of results for the condition of uniform heat input.

Also shown in figure 5 is the variation of effective heater power density (input power minus loss to the cone interior) with surface distance from the nose. The decrease in effective heater power density with increasing surface distance is indicative of the heat loss to the cone interior since the input density was essentially uniform. The internal heat loss ranged from a minimum of approximately 3 percent to a maximum of about 10 percent of the total heat input. The rate of heat loss to the cone interior increased steadily with increasing surface distance from the nose except for heaters A and B, where measured temperatures indicated negligible internal heat loss in all cases.

The theoretically predicted curves of convective heat-transfer coefficient h for both laminar and fully turbulent flow are presented for comparison with experimental results. Also shown are the predicted values of stagnation heat transfer determined from references 7 and 8.

Turbulent heat transfer. - For the turbulent flow region, the lower curve (fig. 5) represents the two-dimensional (flat-plate) heat transfer, and the upper curve represents the predicted heat transfer for three-dimensional flow for a cone. The turbulent heat-transfer results ($s > 4.0$) fall between the two predicted curves but, for the most part, are only slightly greater than the values predicted for the flat plate; only in the forward region of turbulent flow do the data tend toward agreement with the values predicted for the cone. The order of agreement between the experimental and the predicted values shown in figure 5 is typical for all the heat-transfer data obtained.

From theoretical considerations (ref. 6), the turbulent heat transfer from the surface of a cone with zero pressure and temperature gradients is expected to be approximately 15 percent greater than that from a flat plate. Because the surface area of a cone increases rapidly with increasing surface distance, a comparative thinning of the boundary layer or decreased rate of boundary-layer growth occurs, with a consequent expected increase in rate of heat transfer over that experienced for a two-dimensional body, other conditions being identical. The experimental data do not provide verification of this expected increase in heat transfer for reasons that are not readily apparent. The results of references 10 and 11 indicate that, for a flat plate with a turbulent boundary layer, both a positive temperature gradient (increasing temperature with increasing surface distance) and a negative pressure gradient (decreasing pressure with increasing surface distance) tend to increase local heat transfer over that obtained for conditions of uniform temperature and zero pressure gradient. Since the effects of both these gradients are contained in the experimental data of figure 5 (for $s > 4.0$), corrections to the data would yield results that are directly opposite to obtaining closer agreement between the experimental and the predicted heat transfer for the cone. The lack of agreement between the measured and the predicted heat transfer cannot be attributed, therefore, to temperature or pressure gradient effects. Thorough checks of the experimental techniques and procedures failed to disclose any source of consistent error. To eliminate the possibility of error in the measurement of heat loss to the cone interior, calculations were made for assumed zero heat loss to the interior of the cone. These results were not significantly greater than those presented in figure 5.

Stagnation heat transfer. - The experimental heat-transfer results for the stagnation region of the cone were consistently much lower than those predicted from the theoretical and experimental studies of references 7 and 8. This is believed to be due almost entirely to heat conduction effects occurring within the nose region (heater A). Figure 5 indicates the magnitude of these effects. For all conditions investigated, the heat-transfer coefficients for the nose section were nearly constant, which would not normally be expected for a body of this shape (spherical nosecap followed by a conical afterbody). It appears that

conduction effects were sufficient to yield stagnation values of heat transfer that were not local values but rather an approximate average of the local values of heat transfer that would have existed over the nosecap in the absence of conduction effects.

Laminar heat transfer and transition. - Another important result of the investigation was the very limited extent of laminar boundary-layer flow on the cone, as evidenced by the data in figure 5. A comparison of the experimental data with the predicted values of Drake (ref. 3) for the nose region indicates that little laminar flow exists and that transition begins very early.

The data of figure 5 are replotted in figure 6 in terms of nondimensional parameters; the correlation between the various sets of data is good over the entire range of Reynolds number investigated. When plotted in this form, the data show perhaps more clearly the limited extent of the laminar flow region and the low values of Reynolds number at which transition was initiated and completed. (From flat-plate analyses, transition would not be expected to occur at values of Re_s less than approximately 5.0×10^5.) The data points at $Re_s = 7.3\times10^4$ represent a surface distance of only 0.5 inch from air stagnation; immediately downstream, at a surface distance of 1.0 inch ($Re_s = 1.5\times10^5$), the boundary layer appears to be in transition. Since the peak in the velocity-distribution curve (see fig. 4(a)) occurs at a surface distance of approximately 0.7 inch ($Re_s = 1.1\times10^5$ in fig. 6) from stagnation, the initiation of transition must be associated in some manner with this abrupt change from a highly favorable to an adverse pressure gradient. This abrupt change in pressure gradient results from the basic phenomenon of flow about a spherically capped body (nosecap).

The location of transition may perhaps be better understood if the flow about the nose of the model is assumed to approximate that about a sphere. Experimental data (ref. 12) indicate that the boundary layer over a sphere may be entirely laminar up to Reynolds numbers (based on sphere diameter) of 1.0×10^5 to 4.0×10^5, with laminar separation occurring at approximately 83° from stagnation. The value of critical Reynolds number within this range at which the boundary layer ceases to be entirely laminar is dependent on the degree of stream turbulence and surface roughness present. Since it is known that stream turbulence in the icing tunnel is appreciable and that the spinner nose is not an entirely smooth surface, an entirely laminar boundary layer would be expected to exist only for the lower values of critical Reynolds number (near 10^5). In this investigation, the Reynolds number Re_d based on the 1-inch diameter of the nosecap ranges from 1.8×10^5 to 2.6×10^5. Thus, on the basis of approximating the flow about the nose of the model by that about a sphere, the critical Reynolds number is exceeded, and transition would be expected to occur forward of the 83° station for all conditions. On the present model, however, the hemispherical nosecap extends to only about 75° from

stagnation, at which point it attaches to the conical body. Hence, for the data presented in figure 6 ($Re_d \approx 1.8\times10^5$), the maximum extent of laminar flow probably cannot exceed $Re_s \approx 10^5$ (local surface Reynolds number corresponding to 75° on the nosecap). Although initiation of transition appears to result from the nature of the flow about the nosecap, the abrupt change in pressure gradient probably destabilizes the boundary layer further and thus completes transition in a relatively short distance. For higher free-stream velocities, the laminar region may be expected to be even less than that noted for the data in figure 6.

Because the region of laminar flow was extremely small, the heat-transfer results for this region were limited to data obtained from a single measuring station (data for $Re_s = 7.3\times10^4$, fig. 6). These data cannot adequately describe the heat transfer in the laminar region and, hence, the order of agreement between experimental and predicted results cannot be definitely stated. Although the results appear to agree quite well with predicted values, this fact may be fortuitous in view of the nature of the heat-transfer results previously described for the nose section, that is, essentially constant values of heat-transfer coefficient and surface temperatures. Because the measured surface temperatures were always practically constant for heater A area (even for the case of uniform heat input), the theoretical results of reference 3 were determined on the basis of uniform surface temperature only.

Effects of stream velocity on transition and heat transfer. - Data showing the effect of change in free-stream velocity on temperature distribution and heat-transfer characteristics are presented in figure 7 for constant operating conditions. The curves for surface temperature rise and for convective heat-transfer coefficient are very similar, with no particular trends apparent other than an expected change in magnitude accompanying the change in free-stream velocity.

The data of figure 7, replotted in terms of dimensionless parameters in figure 8, show single-curve correlation over the entire experimental range. The fact that the data correlate in the transition region indicates that transition is initiated at a relatively constant value of Reynolds number and, hence, a forward movement of transition occurs at the higher free-stream velocity. This forward movement in transition with increasing stream velocity is in accordance with the characteristics of flow about a sphere or a spherically capped body. For all conditions investigated, initiation of transition was found to occur at a local surface Reynolds number of the order 8.0×10^4. Transition from laminar to fully developed turbulent flow was completed at values of Reynolds number less than 5.0×10^5. By way of comparison, the corresponding minimum Reynolds numbers for an ellipsoidal body investigated in the same tunnel (ref. 1) were 0.8×10^6 and 3.0×10^6 for the initiation and completion of transition, respectively (a 10- and 6-fold variation in Re_s).

4274

CR-2 back

Heat-conduction effects. - The solid data points in figures 7 and 8 are heat-transfer coefficients h_{av} corrected for skin-conduction effects (longitudinal direction only) by the method of reference 1. These data are typical of all the data obtained for uniform heat input. The heat-transfer coefficients for each heater segment were not significantly different from the measured effective local values except in the region where the steepest temperature gradient existed (principally heater segment B). Although segment B gained heat by conduction from both segments A and C, as evidenced by the surface temperature distribution in figure 7, the change resulting from skin-conduction corrections was of the order of 9 percent. The over-all skin-conduction effects (longitudinal direction only) are considered to be small; therefore, all subsequent heat-transfer data are given only in terms of measured effective local coefficients.

Effects of rotation and angle of attack. - The heat-transfer results for a spinner rotational speed of 1200 rpm are presented in figure 9. The data were obtained at two values of free-stream velocity and angles of attack of 0° and 6° for uniform heat input. The data for stationary operation at 0° angle of attack are shown for comparison. Rotational speeds as high as 1200 rpm had no discernible effect on heat transfer for the range of angle of attack and free-stream velocity studied. This result might be anticipated because the local surface velocities measured with rotation at 0° angle of attack were, at a maximum, only 5 percent greater than those obtained with zero rotation. (See figs. 4(a) and (b).) At angles of attack other than 0°, the averaging effect of rotation yields heat-transfer results that are essentially the same as those obtained for 0°.

Heat-transfer measurements were made on the stationary spinner at meridional locations corresponding to the upper and lower surfaces of the cone at 6° angle of attack. The results are presented in figure 10. In general, for a given Reynolds number, the Nusselt numbers were smaller on the upper surface than on the lower surface, except in the range of Re_s from about 4.0×10^5 to 8.0×10^5 where the values were about the same. At Reynolds numbers greater than about 8.0×10^5, this trend is consistent with the characteristics of flow about bodies of revolution at angle of attack. For conical bodies, all flow streamlines (except those corresponding to the upper- and lower-surface meridionals) follow a somewhat helical path about the body, starting on the pressure side (lower surface) and proceeding circumferentially (and rearwardly) toward the upper, or sheltered, surface. This flow characteristic produces a thinned boundary layer on the pressure side with a consequent increase in heat transfer, and a correspondingly thickened boundary layer on the sheltered side with a reduction in heat transfer. Hence, when the data for angle of attack without rotation are plotted in the Nusselt-Reynolds number form (fig. 10), definite trends with respect to meridional location are observed.

Figure 11 presents the same data for the basic relation of convective heat-transfer coefficient h and surface distance for stationary spinner at angle of attack. The data taken in a meridional plane midway between the upper and lower surfaces are also included. At surface distances greater than approximately 6.0 inches, the coefficients obtained on the sheltered surface were from 6.0 to 13.0 percent less than those obtained for corresponding locations on the pressure, or lower, surface. For surface distances less than 6.0 inches, an opposite trend occurred. However, the factors that govern heat transfer in this region are considered to be of sufficient magnitude to affect the reliability of the results, particularly those for the upper surface.

4274

Heat Transfer with Uniform Surface Temperature Distribution

Typical results obtained for the condition of uniform surface temperature (nonuniform heat input) are presented in figure 12. Data are shown for a stationary and rotating spinner, two values of free-stream velocity, and 0° angle of attack. The surface temperature rise was approximately 100° F in each of the three random tests shown. The experimental results show the same order of agreement with the theoretically predicted values as the data for uniform heat input. The two sets of data obtained at the lower free-stream velocity (283 and 285 ft/sec) for the stationary spinner show the repeatability of the data to be within 10 percent. Although the data have slightly more scatter than that obtained for corresponding conditions with uniform heat input, the results appear to provide good representation of the heat-transfer mechanism. As was the case with uniform heat input, the data for uniform surface temperature indicate no measurable effects of rotation on the spinner heat-transfer characteristics. No data were obtained for the stationary spinner at angle of attack.

A replot of these data in terms of the Nusselt-Reynolds number parameters in figure 13 shows good correlation between the various sets of data. In general, the heat-transfer results obtained with uniform surface temperature are practically identical to those obtained with uniform heat input.

SUMMARY OF RESULTS

An experimental wind-tunnel investigation of heat transfer from the surface of a conical forebody (18.9-in. maximum diameter) operating under stationary, rotating, and angle-of-attack conditions yielded the following results:

1. Good correlation of the heat-transfer results was obtained by use of the Nusselt-Reynolds number relation for the complete operating range

investigated for 0° angle of attack with and without spinner rotation, and for angles of attack up to 6° with rotation.

2. Rotational speeds up to 1200 rpm had no apparent effect on the heat-transfer characteristics of the spinner. The heat-transfer data at angle of attack with rotation were essentially the same as those obtained at 0° angle of attack without rotation.

3. Heat-transfer results in the region of turbulent boundary-layer flow were consistently in closer agreement with the values predicted for two-dimensional bodies than with those predicted for a cone.

4. For stationary operation at 6° angle of attack, the measured values of heat-transfer coefficient in the turbulent region were from 6.0 to 13.0 percent less on the sheltered side (upper surface) than those on the windward side (lower surface) for corresponding surface locations.

5. Early boundary-layer transition occurred for all conditions investigated. Transition was initiated at a fairly constant value of local Reynolds number (based on surface distance from nose) of 8.0×10^{4}. In all cases, the transition from laminar to turbulent flow was completed at Reynolds numbers less than 5.0×10^{5}.

Lewis Flight Propulsion Laboratory
National Advisory Committee for Aeronautics
Cleveland, Ohio, July 25, 1957

REFERENCES

1. Lewis, James P., and Ruggeri, Robert S.: Investigation of Heat Transfer from a Stationary and Rotating Ellipsoidal Forebody of Fineness Ratio 3. NACA TN 3837, 1956.

2. von Glahn, U.: Preliminary Results of Heat Transfer from a Stationary and Rotating Ellipsoidal Spinner. NACA RM E53F02, 1953.

3. Drake, Robert M., Jr.: Calculation Method for Three-Dimensional Rotationally Symmetrical Laminar Boundary Layers with Arbitrary Free-Stream Velocity and Arbitrary Wall-Temperature Variation. Jour. Aero. Sci., vol. 20, no. 5, May 1953, pp. 309-316.

4. Eckert, E. R. G.: Introduction to the Transfer of Heat and Mass. McGraw-Hill Book Co., Inc., 1950, p. 156.

5. Van Driest, E. R.: Turbulent Boundary Layer in Compressible Fluids. Jour. Aero. Sci., vol. 18, no. 3, Mar. 1951, pp. 145-161.

6. Van Driest, E. R.: Turbulent Boundary Layer on a Cone in a Supersonic Flow at Zero Angle of Attack. Jour. Aero. Sci., vol. 19, no. 1, Jan. 1952, pp. 55-57; 72.

7. Sibulkin, M.: Heat Transfer Near the Forward Stagnation Point of a Body of Revolution. Jour. Aero. Sci., vol. 19, no. 8, Aug. 1952, p. 570.

8. Xenakis, G., Amerman, A. E., and Michelson, R. W.: An Investigation of the Heat-Transfer Characteristics of Spheres in Forced Convection. WADC Tech. Rep. 53-117, Wright Air Dev. Center, Wright-Patterson Air Force Base, Apr. 1953. (Contract AF 33(600)-8114, RDO No. 560-74.)

9. Torgeson, W. L., and Abramson, A. E.: A Study of Heat Requirements for Anti-Icing Radome Shapes with Dry and Wet Surfaces. WADC Tech. Rep. 53-284, Wright Air Dev. Center, Wright-Patterson Air Force Base, Sept. 1953. (Contract AF 33(616)-85, RDO No. 664-802.)

10. Rubesin, Morris W.: The Effect of an Arbitrary Surface-Temperature Variation Along a Flat Plate on the Convective Heat Transfer in an Incompressible Turbulent Boundary Layer. NACA TN 2345, 1951.

11. Tucker, Maurice: Approximate Turbulent Boundary-Layer Development in Plane Compressible Flow Along Thermally Insulated Surfaces with Application to Supersonic-Tunnel Contour Correction. NACA TN 2045, 1950.

12. Kuethe, A. M., and Schetzer, J. D.: Foundations of Aerodynamics. John Wiley & Sons, Inc., 1950.

4274

TABLE I. - DIMENSIONS OF SPINNER

HEATER SEGMENTS

Heater segment	Surface distance from nose, s, in.	Segment surface area, sq in.
A	0 to 2	5.5
B	2 to 5	[a]24.2
C	5 to 9	[a]58.7
D	9 to 16.5	[a]188.8
E	16.5 to 24.5	[a]302.2
F	24.5 to 33	[a]424.4
G[b]	2 to 16.5	30.8
H[b]	16.5 to 33	35.1

[a]Includes parting-strip area per heater segment.

[b]Parting strips.

4274

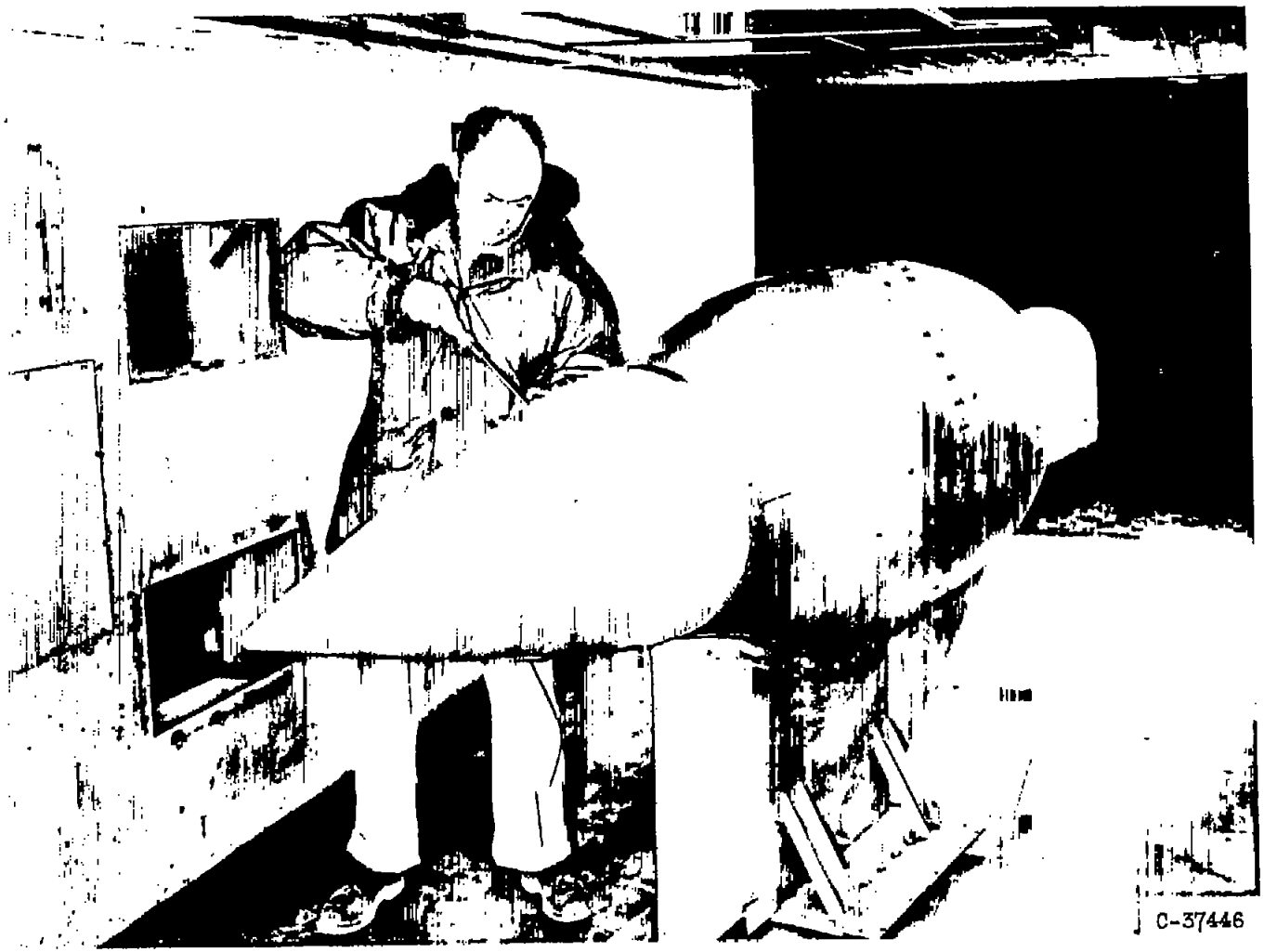

Figure 1. - Installation of conical spinner model in icing research tunnel.

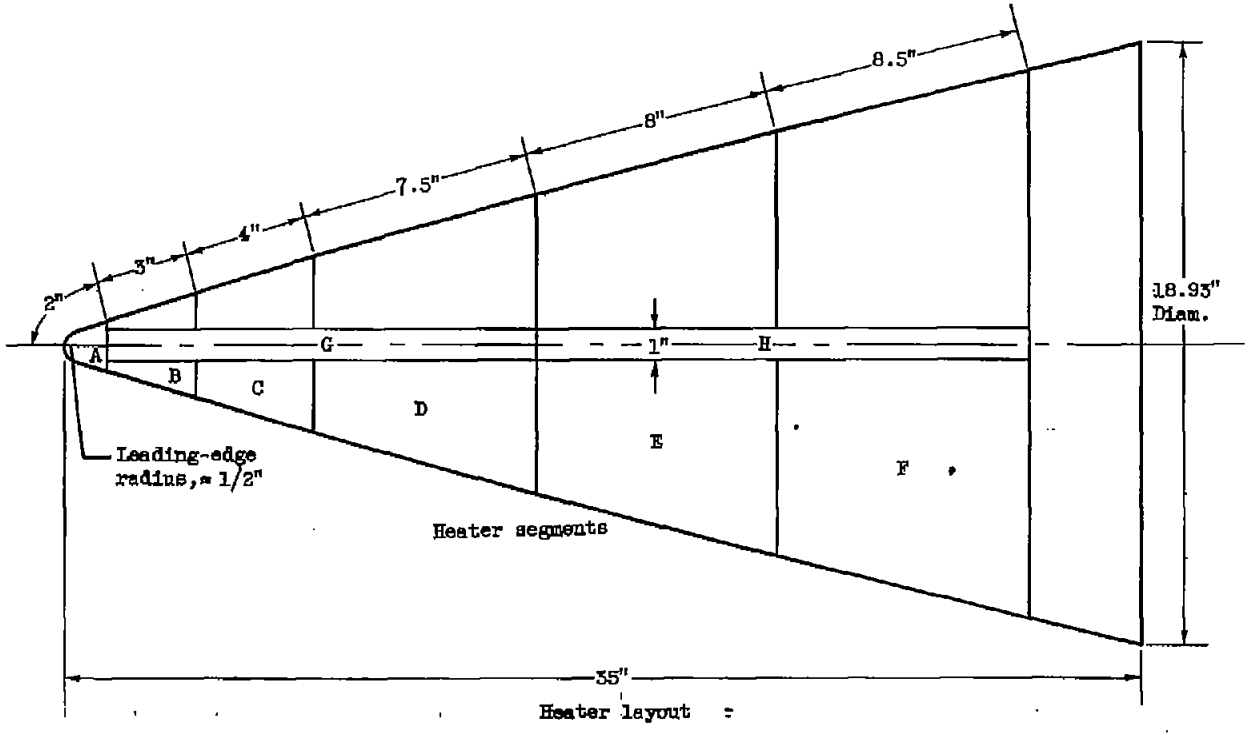

Heater layout

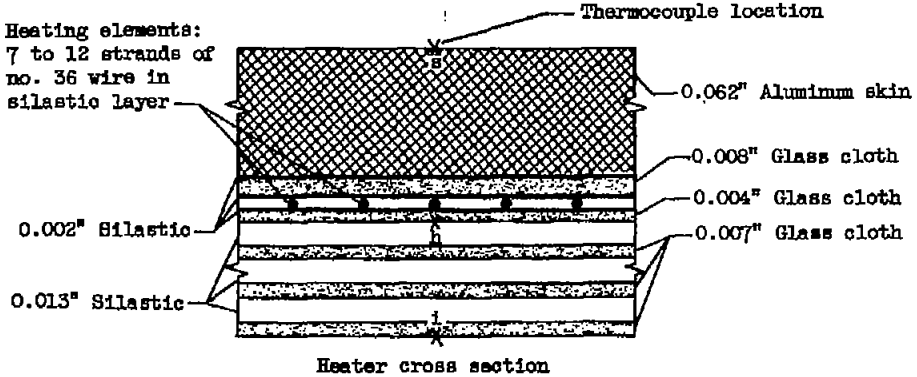

Heater cross section

Figure 2. - Spinner contour and heater details.

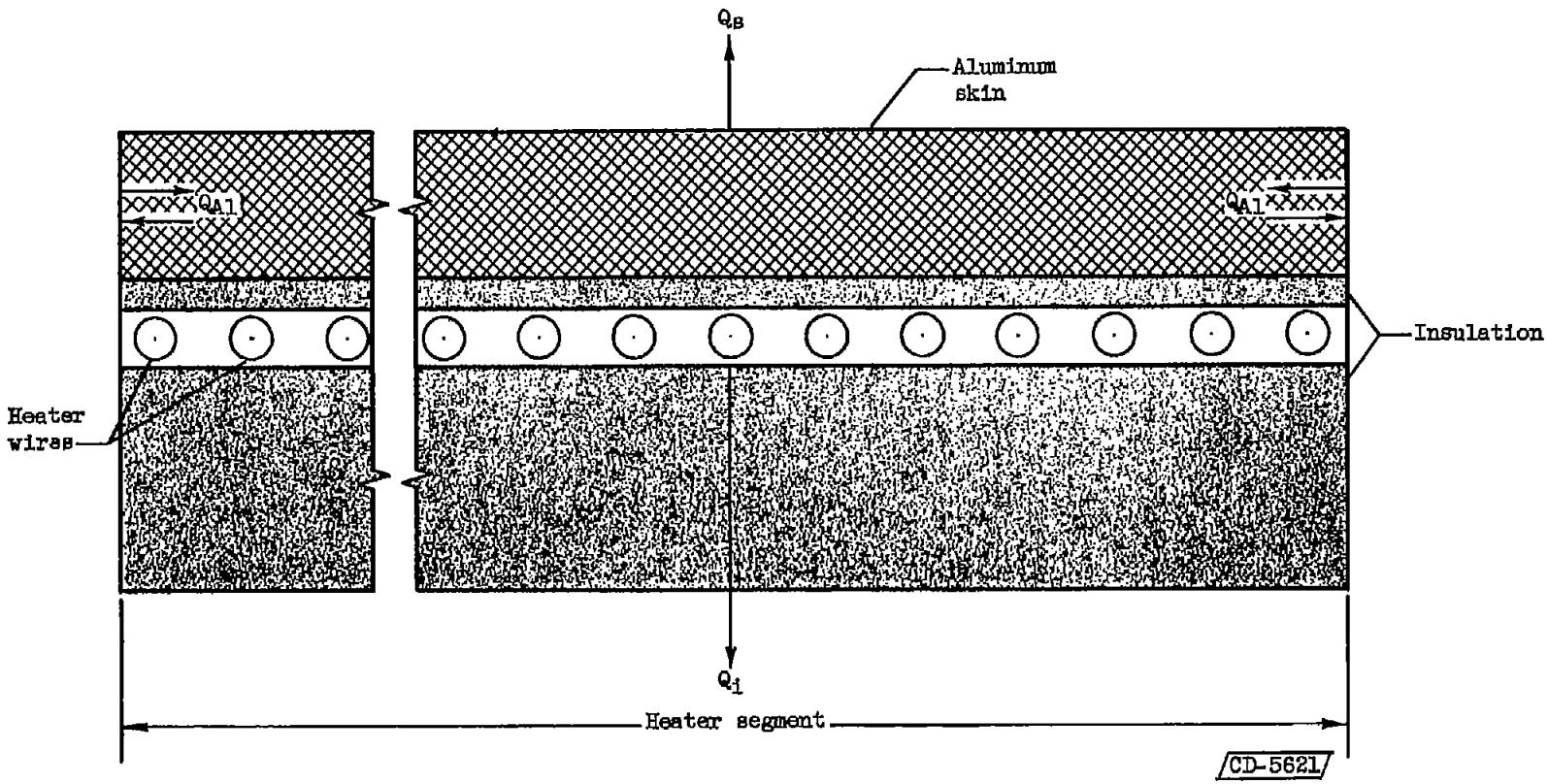

Figure 3. - Simplified heat conduction path used in determination of external heat-transfer coefficients.

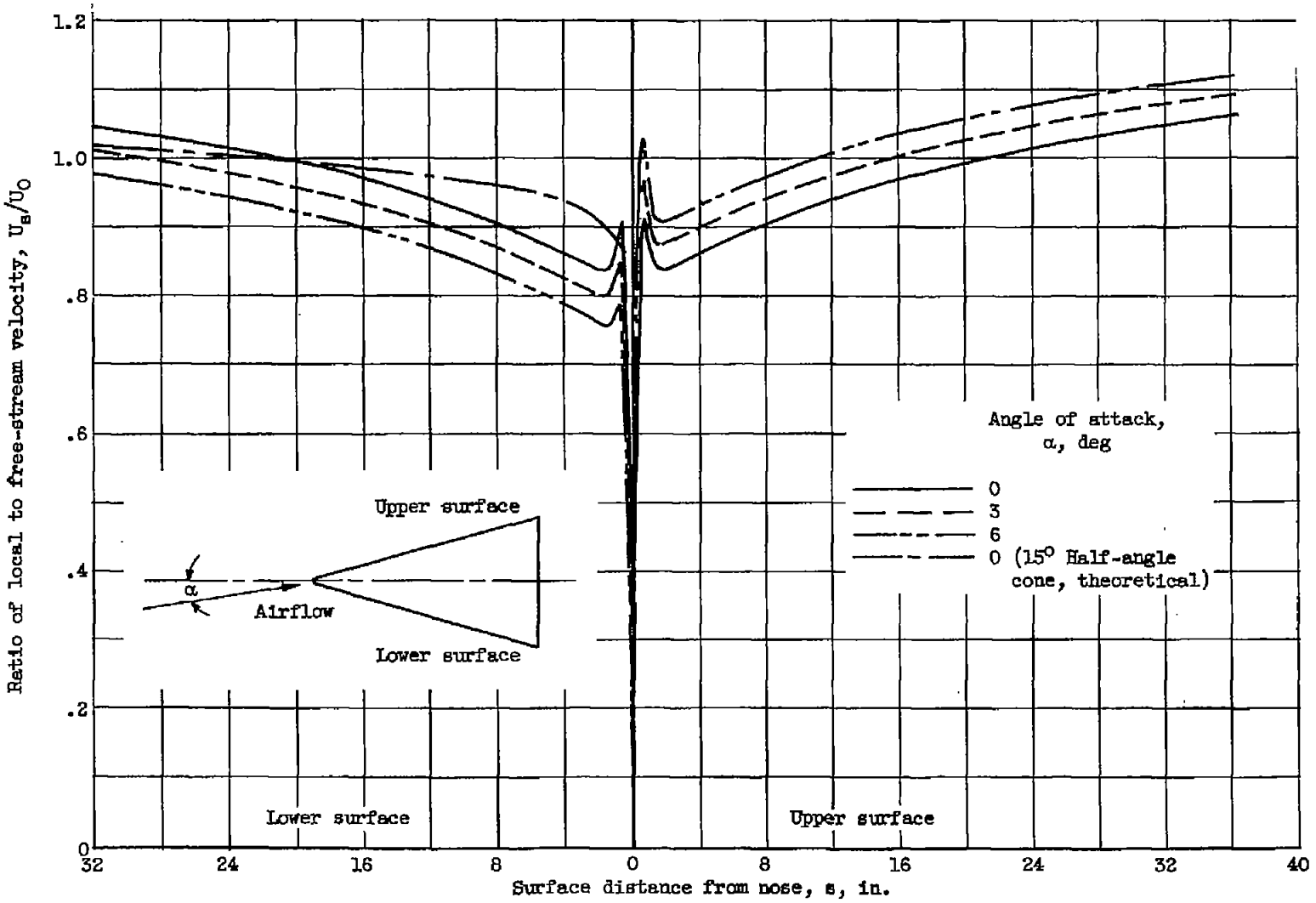

(a) Stationary spinner.

Figure 4. - Velocity distribution over spinner surface.

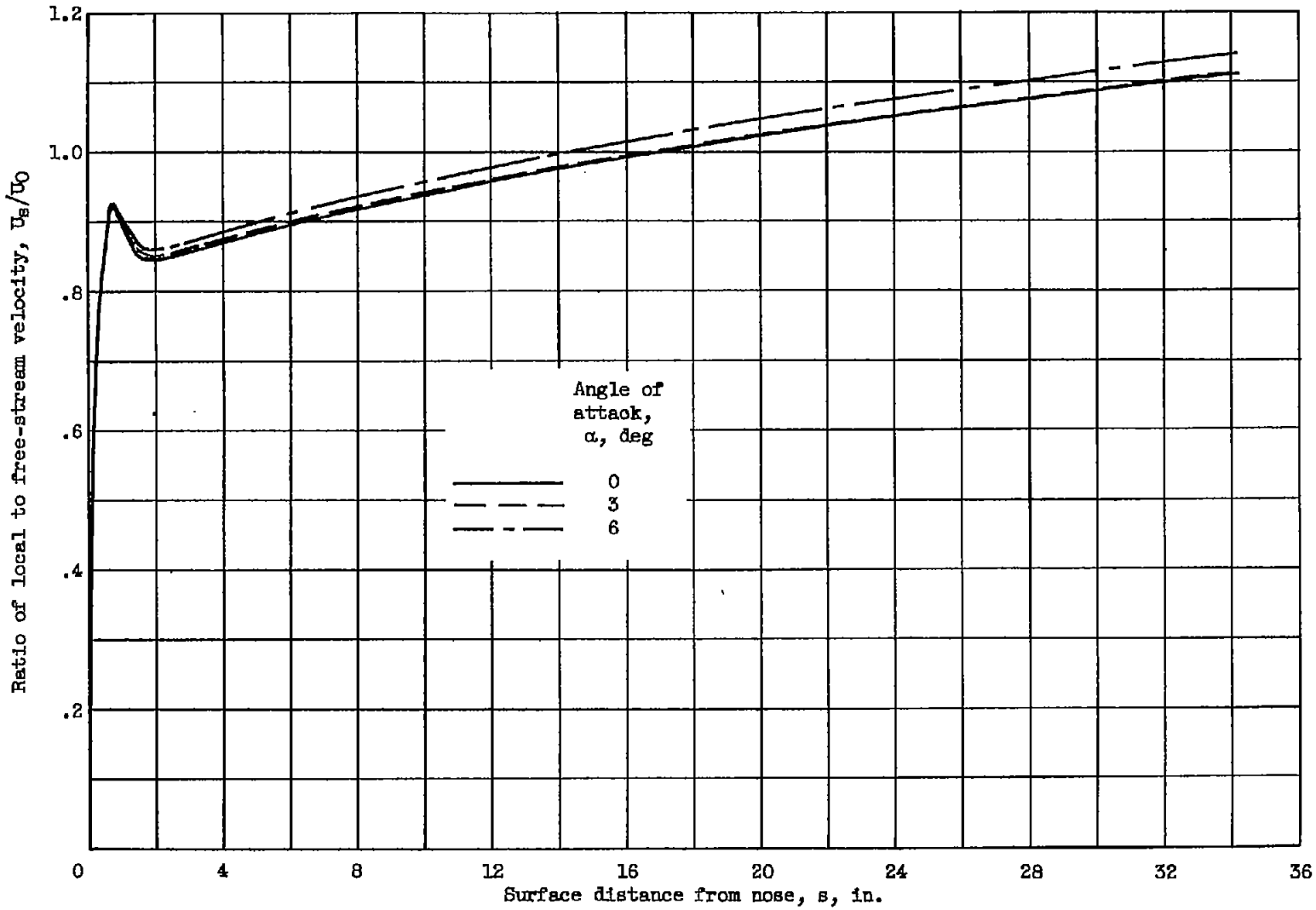

(b) Spinner rotational speed, 1200 rpm; free-stream velocity, 255 feet per second.

Figure 4. - Concluded. Velocity distribution over spinner surface.

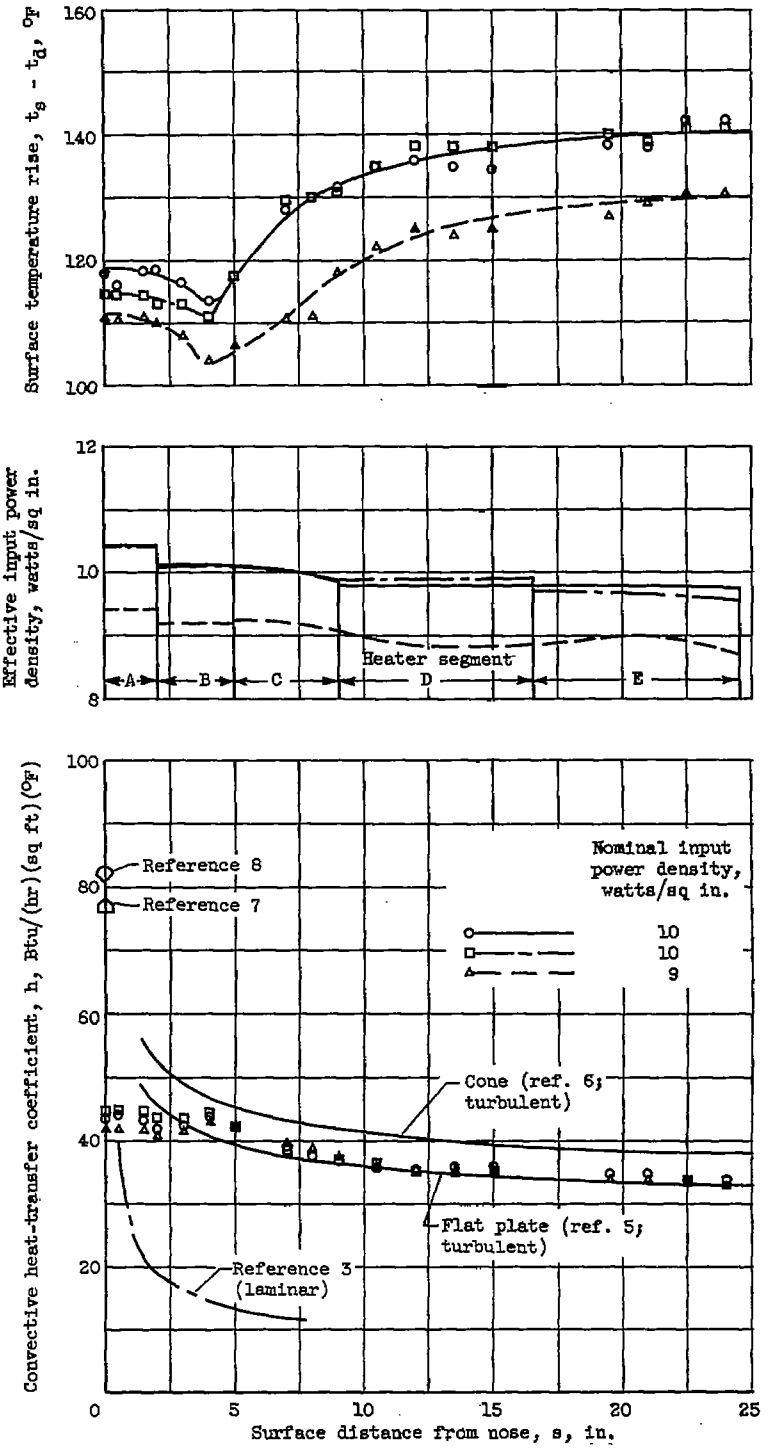

Figure 5. - Variation of surface temperature, effective heater input power density, and convective heat-transfer coefficient for stationary spinner with uniform heat input: Free-stream velocity, 282 feet per second; angle of attack, 0°; average free-stream total temperature, -1° F.

4274

4274

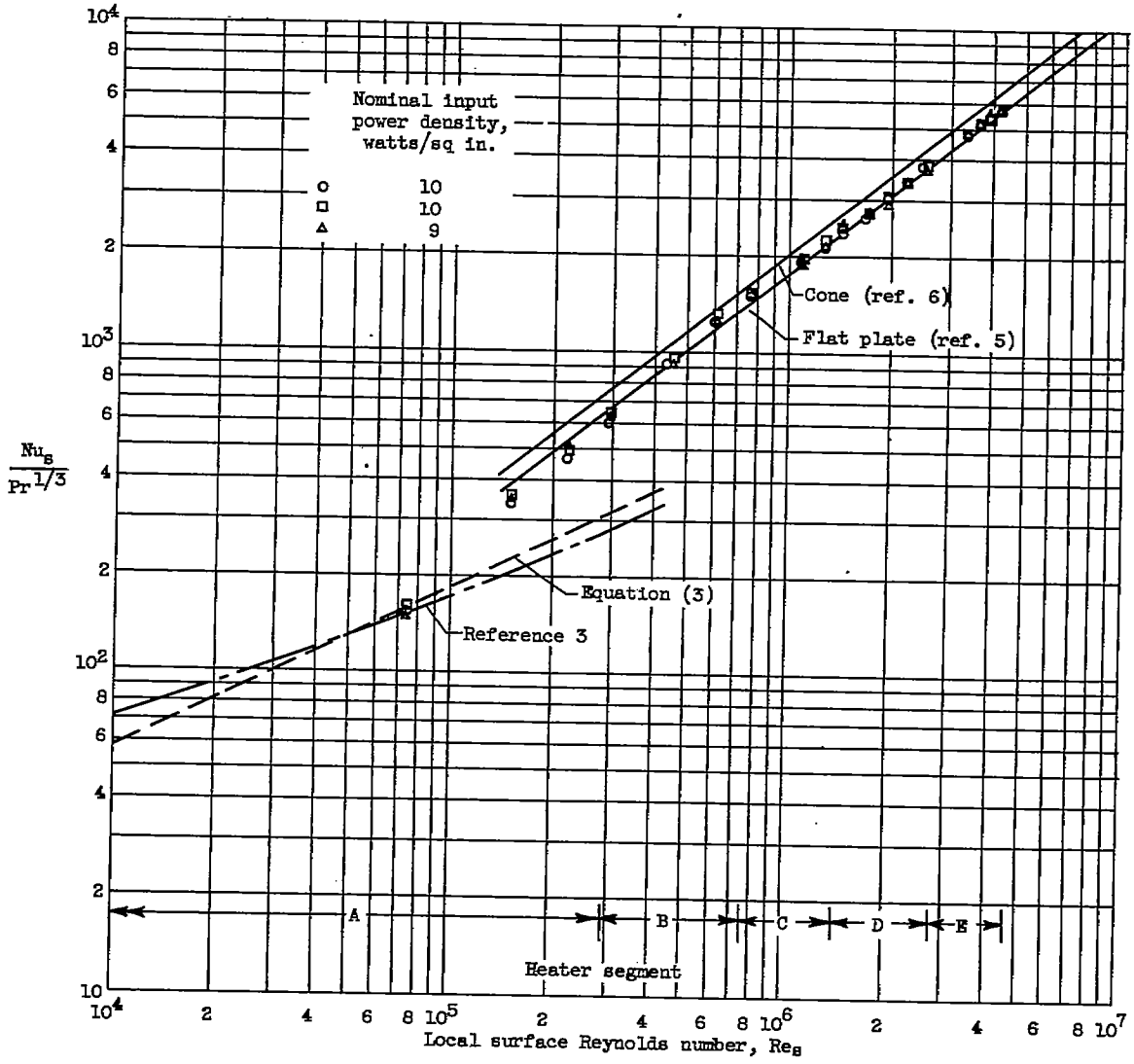

Figure 6. - Correlation of experimental and theoretical heat-transfer results for stationary spinner with uniform heat input. Free-stream velocity, 282 feet per second; angle of attack, 0°; average free-stream total temperature, -1° F.

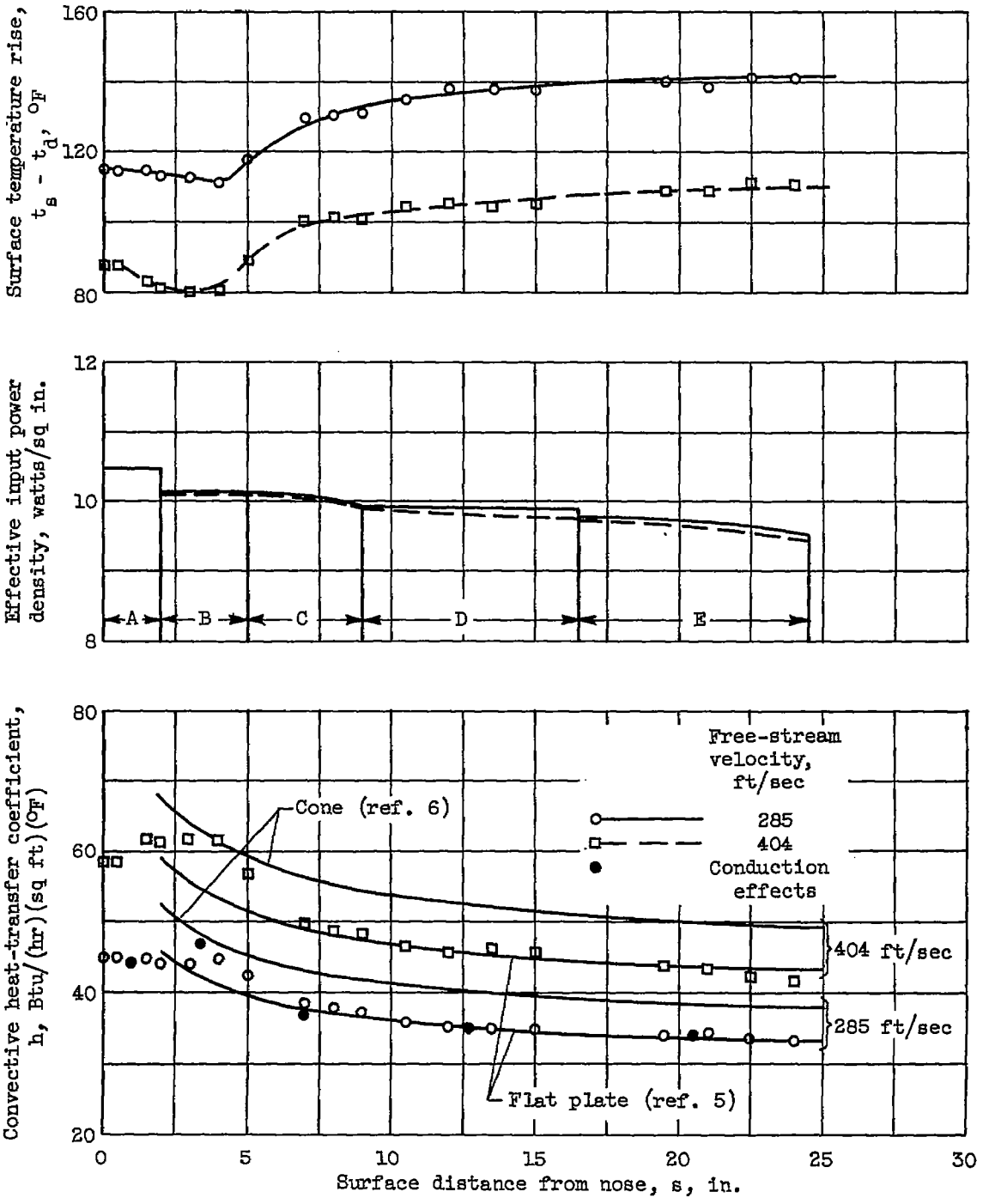

Figure 7. - Effect of free-stream velocity on surface temperature distribution and heat-transfer characteristics of stationary spinner with uniform heat input. Nominal input power density, 10 watts per square inch; angle of attack, 0°; free-stream total temperature, -2° F.

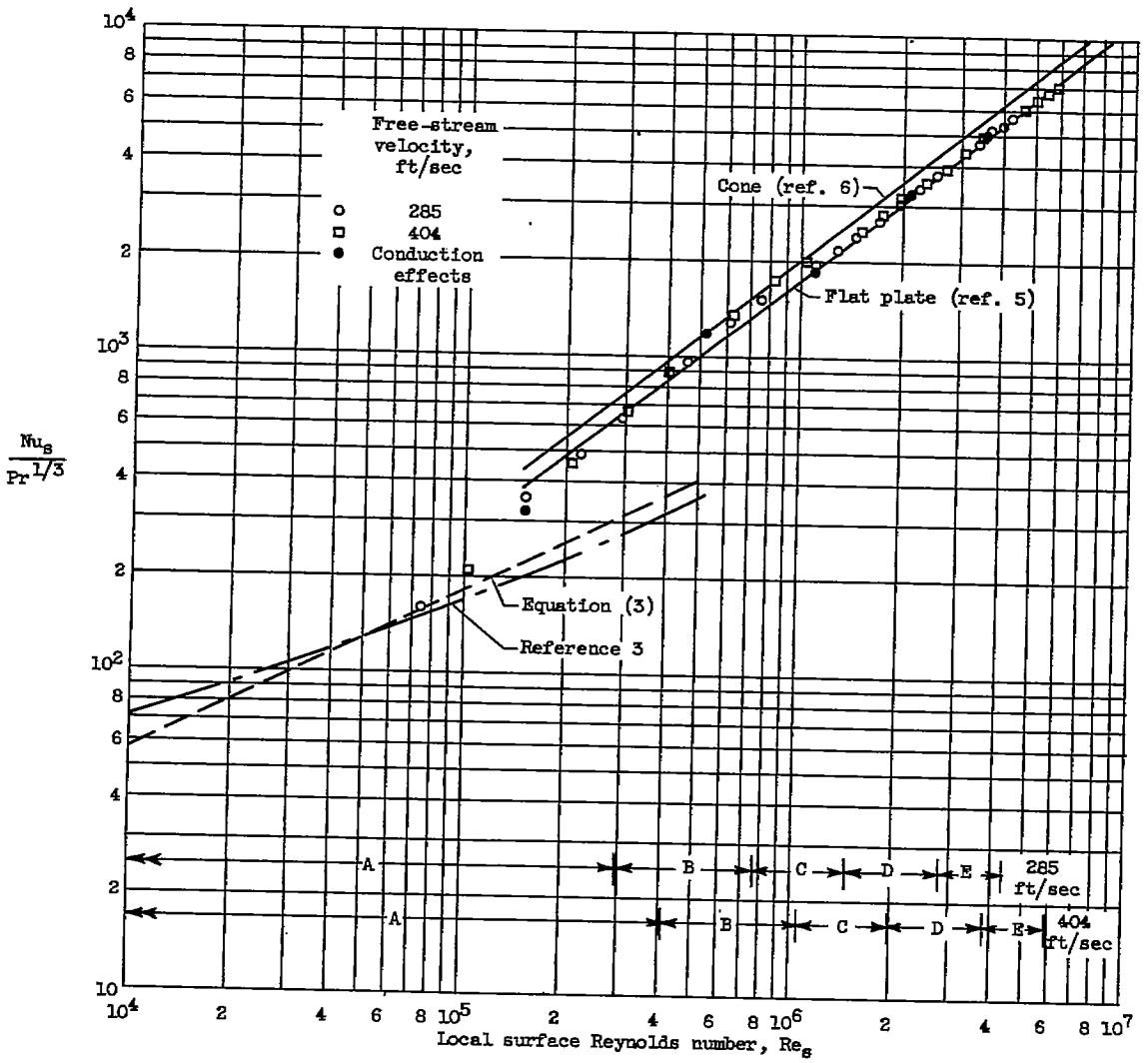

Figure 8. - Correlation of heat-transfer results at two free-stream velocities for stationary spinner with uniform heat input. Nominal input power density, 10 watts per square inch; angle of attack, 0°; free-stream total temperature, -2° F.

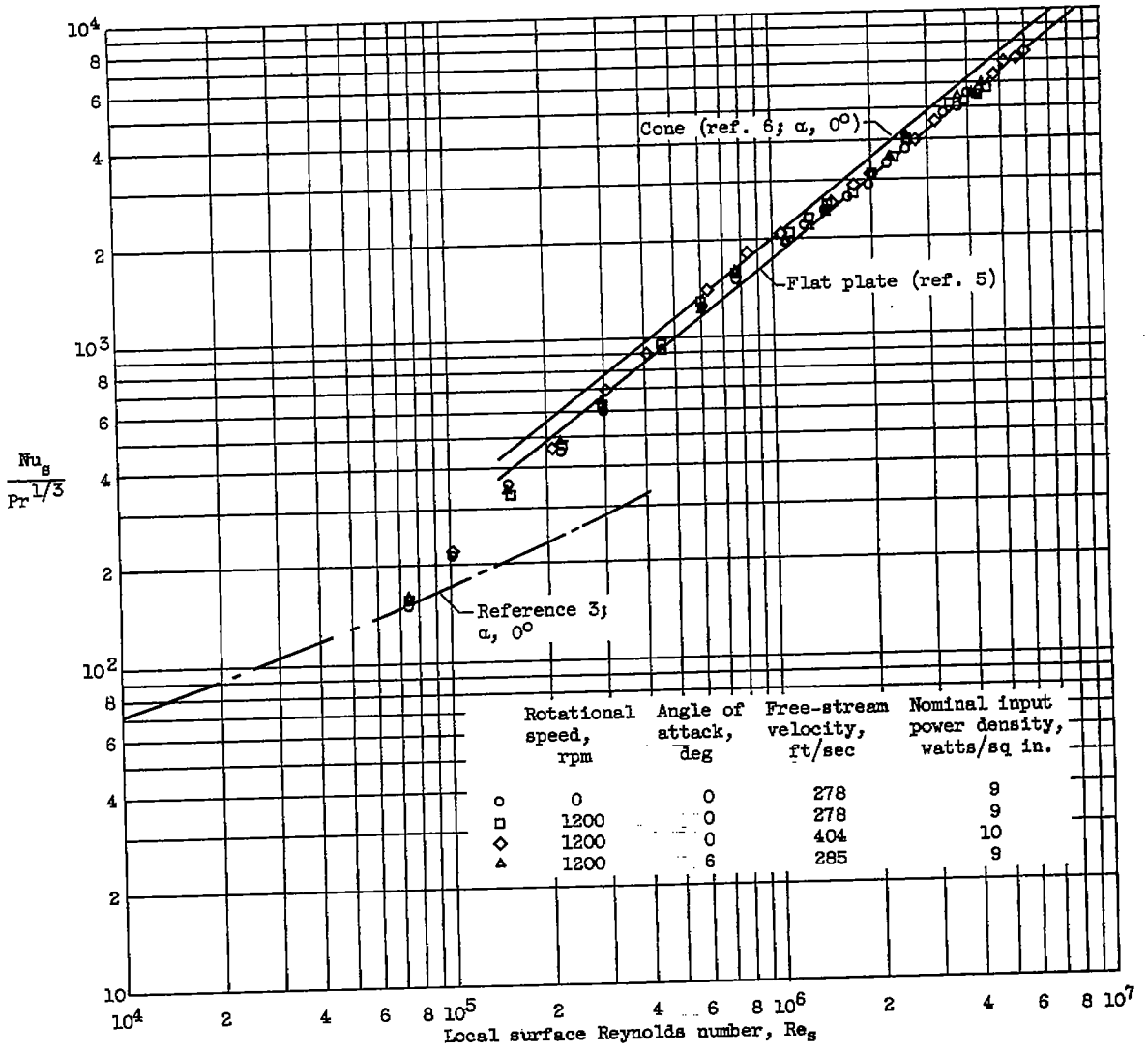

Figure 9. - Comparison of heat-transfer results obtained with stationary and with rotating spinner at various free-stream velocities for 0° and 6° angles of attack. Uniform heat input; average free-stream total temperature, -2° F.

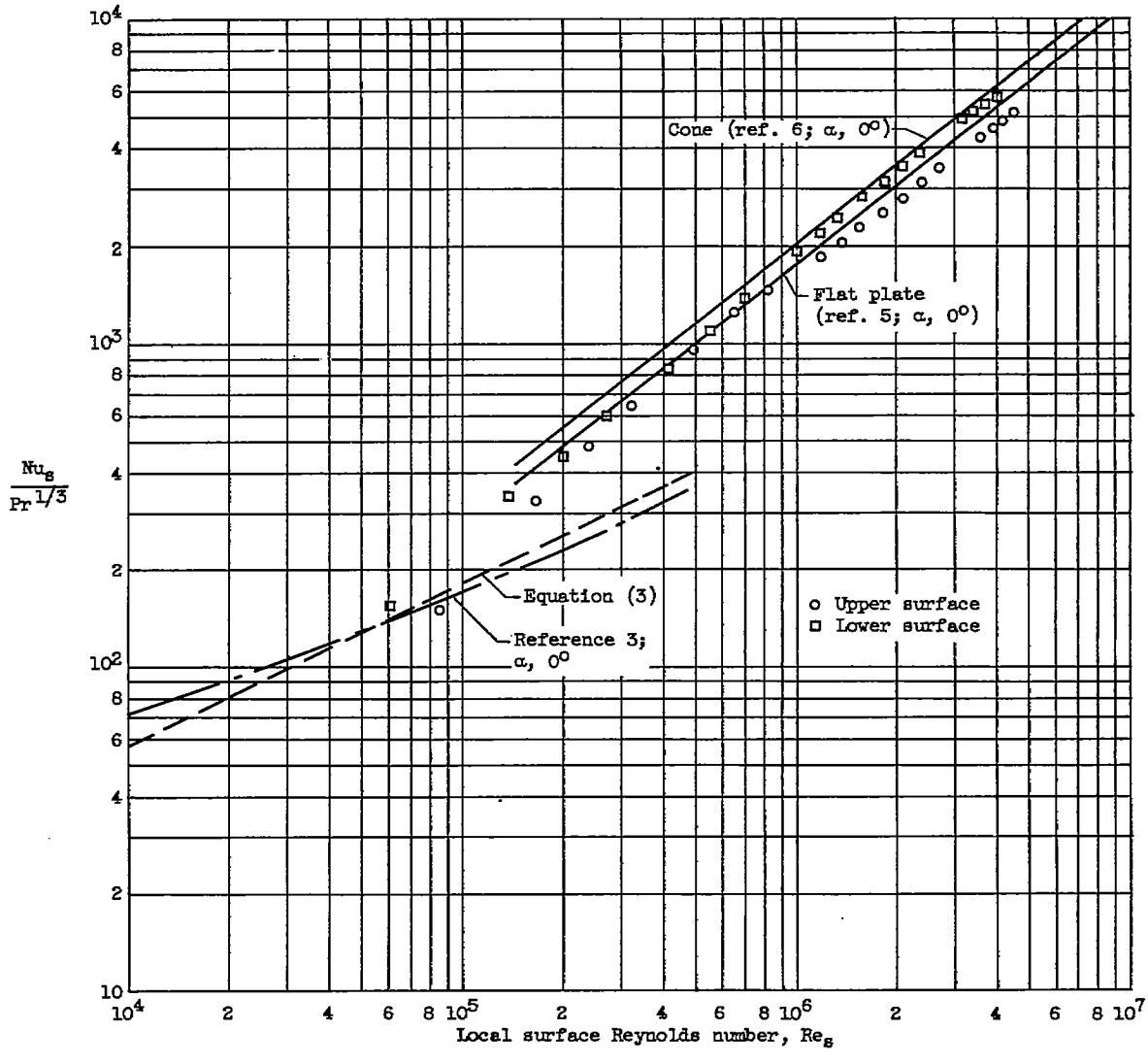

Figure 10. - Heat-transfer data for upper and lower surfaces at 6° angle of attack with stationary spinner. Uniform heat input; free-stream velocity, 284 feet per second; nominal input power density, 9 watts per square inch; free-stream total temperature, 0° F.

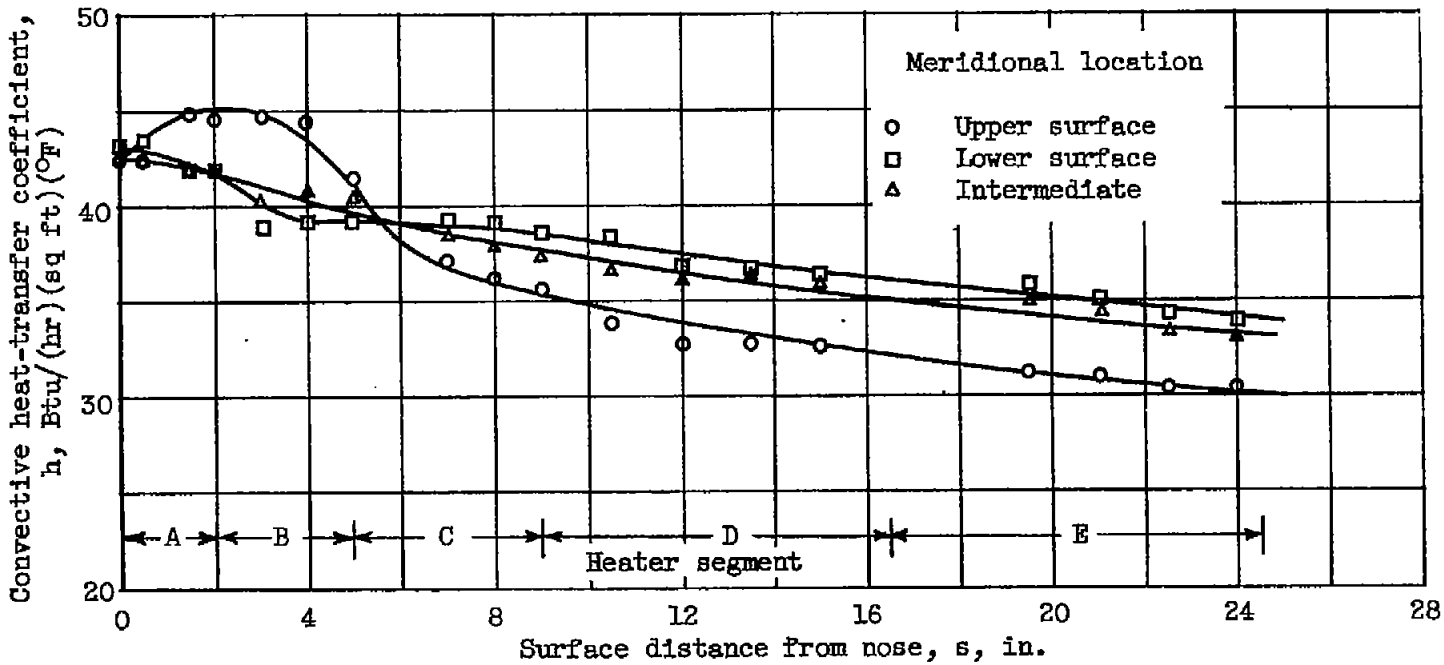

Figure 11. - Comparison of heat-transfer results obtained at three meridional locations on stationary spinner with uniform heat input and at 6° angle of attack. Free-stream velocity, 284 feet per second; nominal input power density, 9 watts per square inch; free-stream total temperature, 0° F.

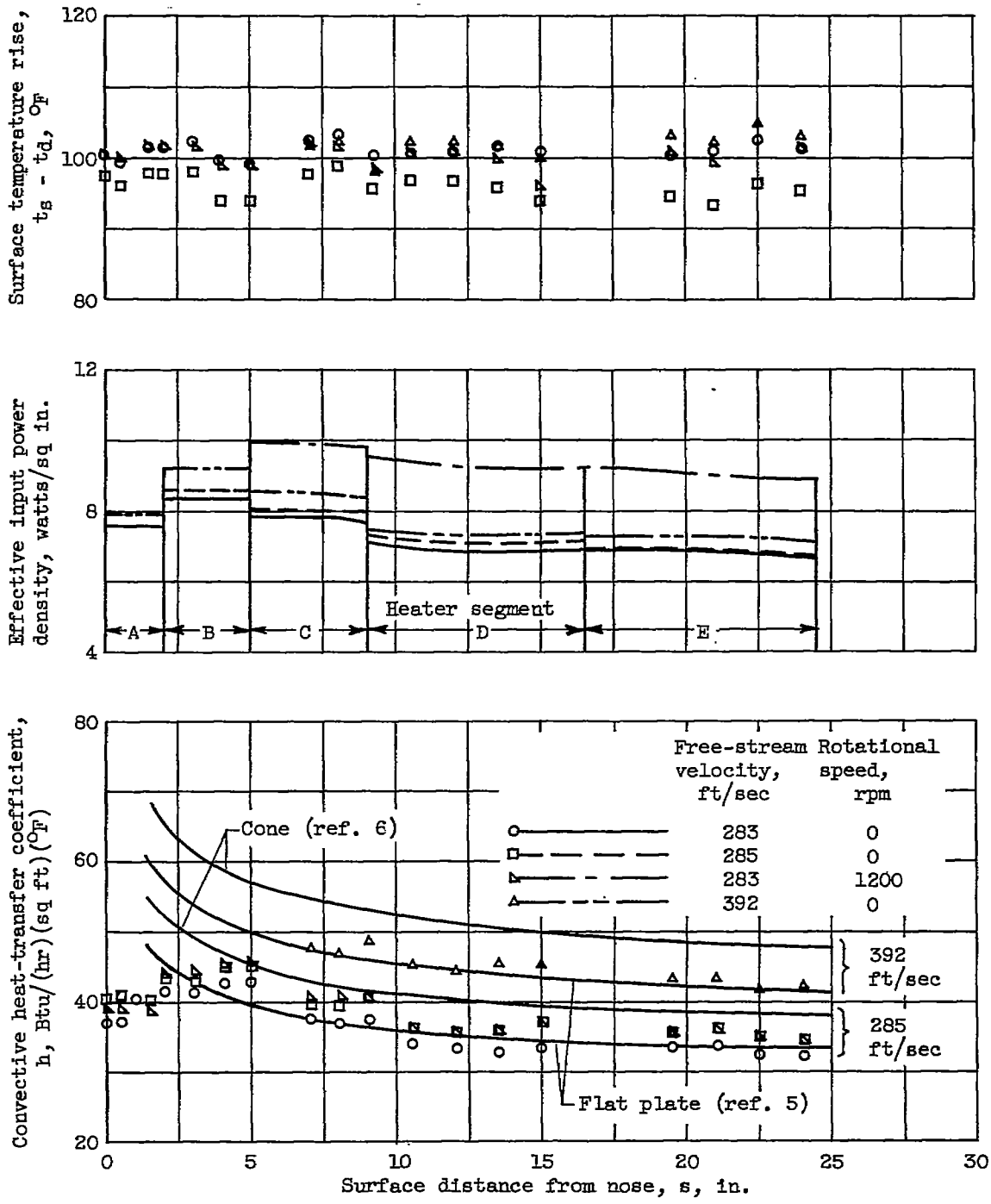

Figure 12. - Experimental results obtained at various free-stream velocities and rotational speeds for spinner with uniform surface temperature. Angle of attack, 0°; average free-stream total temperature, -1° F.

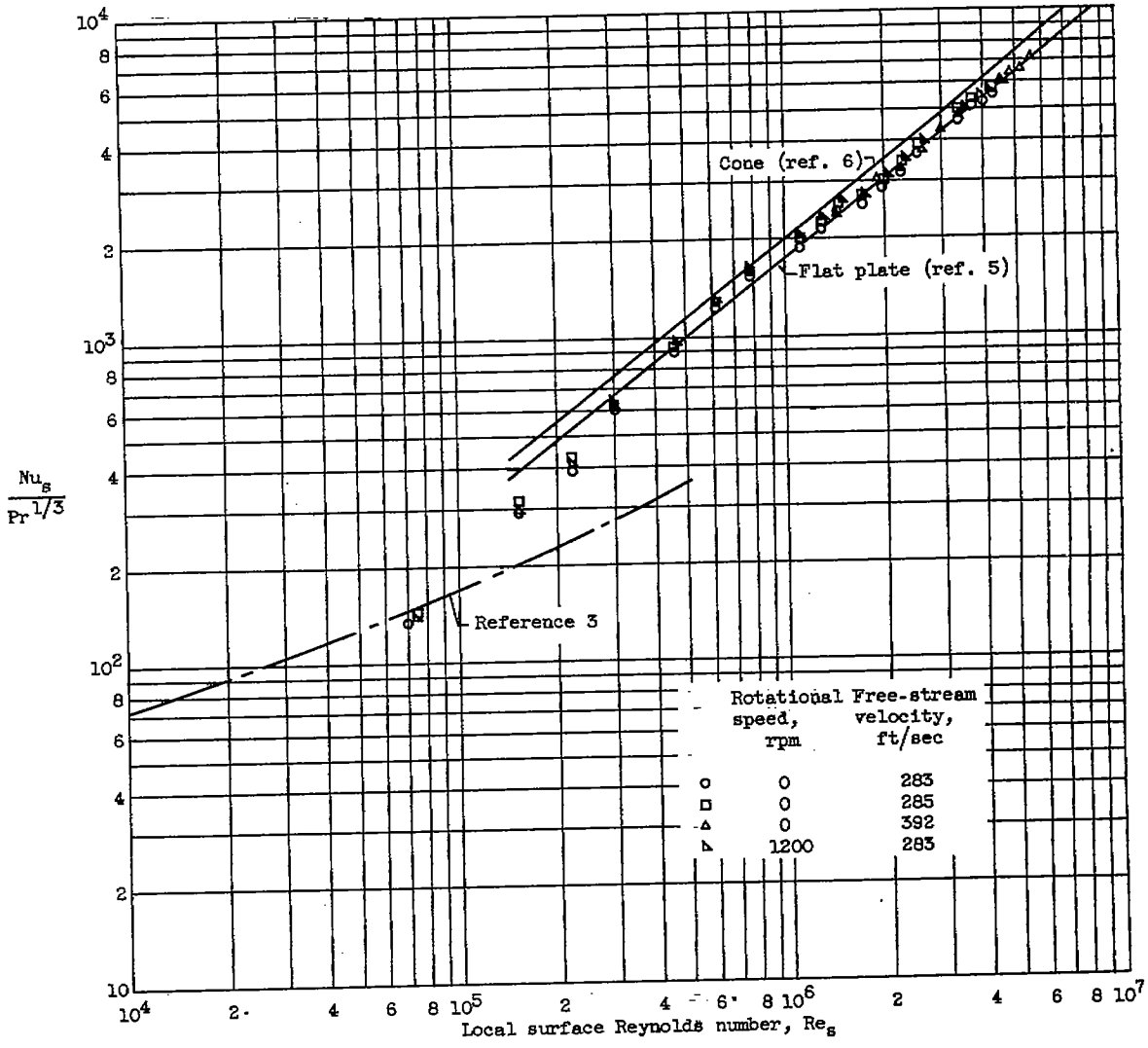

Figure 13. - Correlation of heat-transfer results obtained at various free-stream velocities and rotational speeds for spinner with uniform surface temperature. Angle of attack, 0°; average free-stream total temperature, -1° F.